

On the Origin of Whistler Mode Radiation in the Plasmasphere

James L. Green
NASA/Goddard Space Flight Center
Greenbelt, MD

Scott Boardsen
L3 Communications Analytics Division
NASA Goddard Space Flight Center
Greenbelt, MD

Leonard Garcia
QSS Group, Inc.
NASA Goddard Space Flight Center
Greenbelt, MD

W. W. L. Taylor
QSS Group, Inc.
NASA Goddard Space Flight Center

Shing F. Fung
NASA Goddard Space Flight Center
Greenbelt, MD

B. W. Reinisch
Center for Atmospheric Research
University of Massachusetts, Lowell, MA

Submitted for Publication in *Journal of Geophysical Research*

March 25, 2004

Revised: August 2, 2004

ABSTRACT

The origin of whistler mode radiation in the plasmasphere is examined from three years of plasma wave observations from the Dynamics Explorer and three years from the Imager for Magnetopause-to-Aurora Global Exploration (IMAGE) spacecraft. These data are used to construct plasma wave intensity maps of whistler mode radiation in the plasmasphere. The highest average intensities of the radiation in the wave maps show source locations and/or sites of wave amplification. Each type of emission is classified based on its magnetic latitude and longitude rather than any spectral feature. Equatorial electromagnetic (EM) emissions (~ 30 - 330 Hz), plasmaspheric hiss (~ 330 Hz – 3.3 kHz), chorus (~ 2 kHz – 6 kHz), and VLF transmitters (~ 10 - 50 kHz) are the main types of waves that are clearly delineated in the plasma wave maps. Observations of the equatorial EM emissions show that the most intense region is on or near the magnetic equator in the afternoon sector and that during times of negative B_z (interplanetary magnetic field), the maximum intensity moves from L values of 3 to less than 2. These observations are consistent with the origin of this emission being particle-wave interactions in or near the magnetic equator. Plasmaspheric hiss shows high intensity at high latitudes and low altitudes (L shells from 2 to 4) and in the magnetic equator over L values from 2 to 3 in the early afternoon sector. The longitudinal distribution of the hiss intensity (excluding the enhancement at the equator) is similar to the distribution of lightning: stronger over continents than over the ocean, stronger in the summer than winter, and stronger on the dayside than nightside. These observations strongly support lightning as the dominant source for plasmaspheric hiss, which through particle-wave interactions, maintains the slot region in the radiation belts. The enhancement of hiss at the magnetic equator is consistent with particle-wave interactions. The chorus emissions are most intense on the morning side as previously reported. At frequencies from ~ 10 - 50 kHz VLF transmitters dominate the spectrum. The maximum intensity of the VLF transmitters is in the late evening or early morning with enhancements all along L shells from 1.8 to 3.

1. INTRODUCTION

Whistler mode radiation consists of electromagnetic waves whose upper frequency cutoff is either the local electron plasma frequency (f_p) or gyrofrequency (f_g), whichever is less [Stix, 1992]. Because of the large cold plasma density in the plasmasphere f_p is greater than f_g and supports whistler mode radiation up to frequencies greater than 50 kHz. In the plasmasphere the main whistler mode waves include: equatorial electromagnetic (EM) emissions, plasmaspheric hiss, lightning whistlers, chorus and VLF transmissions. An understanding of the whistler mode emissions in the plasmasphere is important in understanding the dynamics of the radiation belt electrons since the high energy belt particles and the electromagnetic waves in the whistler mode frequency range are believed to strongly interact.

Previous studies of the equatorial EM waves have been limited after first being pointed out by Russell *et al.* [1970]. The EM equatorial waves are believed to play an important role in transferring energy from energetic protons convecting earthward from the plasma sheet, to the thermal plasmaspheric ions flowing along the geomagnetic field lines [Gurnett, 1976; Boardsen *et al.*, 1992]. To date, there has been no systematic spatial distribution study of these waves based on intensity and thereby no real context to understand where in the plasmasphere these potential particle-wave interactions may occur. This study will address this issue.

Plasmaspheric hiss is a broad diffuse band of electromagnetic radiation in the 100s of Hz to 4 kHz frequency range that is confined to the plasmasphere [Taylor and Gurnett, 1968; Russell *et al.*, 1969; and Dunckel and Helliwell, 1969]. Two of the most important characteristics of plasmaspheric hiss are its source location and generation mechanism. Even after three decades of space plasma wave research these two characteristics are still controversial although significant progress has been made in their understanding. This controversy will be explored further in this paper. The last comprehensive review of plasmaspheric hiss was done by Hayakawa and Sazhin [1992].

Lightning generates a very broad emission spectrum. In the kHz frequency range lightning waves are initially trapped in the waveguide formed by the lower ionosphere and ground producing what are called sferics. Under certain conditions, at the atmospheric/ionospheric interface, wave energy can be transmitted through the ionosphere and into the plasmasphere where these waves propagate nearly along geomagnetic field lines in the whistler mode. As they propagate they suffer dispersion giving the well-known "whistler" spectrum [Storey, 1953]. These waves have been observed to directly interact with radiation belt electrons causing them to precipitate [see for example: *Inan et al.*, 1989]. *Sonwalker and Inan* [1989] were the first to observe lightning-generated whistlers triggering hiss emissions. This led these authors to the conclusion that lightning served, to an unknown extent, as an embryonic source of plasmaspheric hiss. This paper will explore the relationship between the distribution of lightning on the Earth with the distribution of plasmaspheric hiss to determine the extent of the hiss/lightning relationship.

Whistler mode chorus emissions are observed extending from the outer regions of the plasmasphere/plasmapause and into the inner magnetosphere. *Sazhin and Hayakawa* [1992] reviewed chorus emissions but a considerable amount of research has been accomplished since then. Much of the new research has explored the interaction with outer radiation belt electrons and chorus observed during substorms [see for example: *Meredith et al.*, 2000 and *Meredith et al.*, 2002]. The spatial extent of these emissions will be explored in this paper and compared to previous results.

A large number of VLF transmitters have been established by a number of countries for the purposes of navigation and communication. The frequencies of these transmitters range from as low as 10 kHz to as high as 50 kHz. Like lightning, transmitter waves also couple through the ionosphere to the magnetosphere and are trapped in the plasmasphere. Transmitter signals are also known to precipitate low energy radiation belt electrons with energies less than 50 keV in the slot region between the inner and outer electron radiation belts [see for example: *Imhof et al.*, 1981; *Vampola*, 1977; *Inan and Helliwell*,

1982]. The spatial extent of VLF transmitter signals found in the plasmasphere will be examined in this study.

In order to perform a comprehensive spatial distribution of these whistler mode emissions a large plasma wave data base has been developed. Very high quality plasma wave measurement data from a variety of instruments are now in the NASA National Space Science Data Center (NSSDC) archive. When properly combined into a 3-D database, these measurements can be used to construct intensity wave maps that yield statistically important source region information that may have been impossible to recognize previously. A similar approach to developing a model of the whistler mode wave activity in the plasmasphere has already been accomplished by *André et al.* [2002] using the same archival DE/PWI data. However, that study did not take into account local time variations in producing latitudinal distributions (see their Figure 4 and 5) and no attempt was made to look for any geographic control of these whistler mode waves indicating a lightning origin.

With the plasma wave intensity map technique, we now have the ability to globally analyze the intensity of plasmaspheric whistler mode waves in a quantitative and systematic fashion, thereby putting into context their spatial distribution and intensity. We will look for "hot spots" in the average wave intensities, thereby identifying source regions and/or sites of plasma wave amplification. The purpose of this paper is to use this new wave map technique to apply a classification scheme for whistler mode waves based on the similarity of their spatial distributions with frequency in a way that has not been presented by earlier studies. This unique approach focuses more on classifying the waves by a common origin rather than previous spectral analysis taken at any one location in the plasmasphere and will more easily provide a method to determine the source region of these whistler mode waves in the plasmasphere.

2. OBSERVATIONS

Observations used in this study are from the plasma wave instrument (PWI) on the Dynamics Explorer-1 (hereafter DE) mission [Shawhan *et al.*, 1981] and the Radio Plasma Imager (RPI) on the Imager for Magnetopause-to-Aurora Global Exploration (IMAGE) mission, [Reinisch *et al.*, 2000].

DE was launched on August 3, 1981 into a polar orbit with initial apogee of 4.65 Earth radii (R_E) geocentric radial distance and 675 km perigee altitude with an orbital period of 6.8 hours. The orbital precession of 108° per year allowed DE to cross the plasmasphere at all local times and nearly all latitudes over a three-year period. Data from the DE/PWI used in this study are from the period September 16, 1981 to June 23, 1984. DE/PWI data was received approximately 40% of the time due to telemetry coverage. The PWI makes spectral measurements over a frequency range from 1.8 Hz to 400 kHz using the sweep frequency receiver (SFR). The measurements are made in 1% frequency bands, logarithmically spaced in frequency. All the DE/PWI data are available in the NSSDC. Four consecutive amplitude measurements for the electric and magnetic wave receivers at each frequency step along with time, frequency, antenna connection and spacecraft position information are available in the archive. Only the second of the four consecutive amplitude measurements are used. The DE/PWI electric field measurements used in this study are all from the 200 m tip-to-tip wire antenna and the 1 m square loop antenna for simultaneous magnetic wave measurements.

The IMAGE spacecraft was launched on March 25, 2000 into a highly elliptical polar orbit with initial geocentric apogee of $8.22 R_E$ and perigee altitude of 1000 km. The RPI instrument on IMAGE is a highly flexible radio sounder that transmits and receives coded radio frequency pulses in the frequency range from 3 kHz to 3 MHz. RPI also makes passive radio measurements (300 Hz bandwidth) that are used in this study. RPI utilizes three orthogonal dipole antennas of 325 m (X-axis), 500 m (Y-axis), and 20 m (Z-axis), all tip-to-tip lengths. The X-axis antenna was 500 m at the beginning of the mission but was shortened to 325 m when it apparently collided with a micro-meteoroid or orbital debris on October 3, 2000. The IMAGE data coverage is from January 1, 2001 to August 6, 2003. Telemetry coverage of RPI was above 95% during this interval. The

IMAGE/RPI and IMAGE orbit data are archived at the NSSDC. Eight consecutive amplitude measurements (3.2 ms/sample) for the electric wave receiver at each frequency step from each antenna along with time, frequency, antenna connection and spacecraft position information are available in the archive. Only the first of the eight consecutive amplitude measurements from the X antenna are used.

The wave map technique used in this study is similar to that used by *Green and Boardsen* [1999] in the study of continuum radiation. The PWI and RPI data were separated into bins of 5° in geomagnetic latitude and 12° in geomagnetic longitude for all radial distances $< 3.5 R_E$, saving the total of the log of the spectral density and total numbers of measurements in each bin for each frequency. No normalization of spectral power densities as a function of radius or distance along a flux tube was attempted. Wave map movies were generated for each frequency for the PWI and RPI data. The data values used for each bin in the wave maps are a weighted sum over that bin and its 8 nearest neighbors of the total spectral density summed over the nine bins divided by the total number of individual measurements summed over the nine bins.

Within the plasmasphere, in addition to radiation in the electromagnetic whistler mode, strong low frequency electrostatic emissions are also prevalent. Only the DE magnetic wave measurements will be used for the whistler mode waves at low frequencies. This will avoid adding the unwanted intensities of electrostatic emissions into the wave survey for those frequencies. This procedure will ensure that only the whistler mode waves are included.

2.1 EQUATORIAL EM EMISSIONS

The average DE/PWI magnetic field spectral densities in the 176.1 Hz band are shown in Figure 1 where panel A is for measurements in the 12.5 – 0.5 MLT meridian plane and panel B is a plot of measurements in the equatorial plane for the same frequency band in solar magnetospheric (SM) coordinates. White pixels indicate no DE measurements. The wave measurements for Figure 1A are sorted by using the sign of the z component of the

interplanetary magnetic field (IMF B_z). It is well known that the IMF B_z parameter is an important factor in the generation of geomagnetic substorms. In panel A, the average magnetic field spectral density is binned according to the absolute value of the magnetic latitude, times the sign of the IMF B_z . Therefore, the +z axis in Figure 1A is the subset of observations for which IMF B_z is positive, while the -z axis is the subset of observations for which the IMF B_z is negative. This method has a number of advantages and is applicable to whistler mode waves due to their expected generation and propagation symmetry about the magnetic equator.

All the characteristic features of the magnetic field spectral density distributions shown in Figure 1A and B are also found over the entire frequency range from ~30-330 Hz. This emission is equatorial EM (fast magnetosonic mode) radiation [Russell *et al.*, 1970; Gurnett, 1976; Boardson *et al.*, 1992] and is found at frequencies between the proton gyrofrequency (f_{gi}) and the lower hybrid frequency (f_{LHR}). Those frequencies are shown on the Figure in blue and green, respectively. Other labels such as the electron gyrofrequency (f_{ge}) are marked in red and also used in the wave maps (not shown in Figure 1). The quantities f_{gi} and f_g are calculated from the measured magnetic field on board DE and from a Tsyganenko [1995] model field for IMAGE. The f_{LHR} is estimated by using the geometric mean of f_{gi} and f_{ge} (which is the upper limit of the lower hybrid). The magnetic field of the EM waves is nearly aligned with the ambient magnetic field, therefore the wave vector is nearly perpendicular to the ambient magnetic field. The wave vector direction combined with the elongated shape of the index of refraction surface along the ambient magnetic field direction strongly confines these waves to the magnetic equatorial region as is demonstrated by cold plasma ray tracing [Boardson *et al.*, 1992].

This study provides, for the first time, a quantitative spatial distribution of the EM equatorial emissions in local time. The distribution of wave spectral densities shown in Figure 1A confirms previous studies of the near equatorial nature of these waves in the outer plasmasphere. In addition, Figure 1A strongly suggests that particle-wave interactions occur within a few tens of degrees of the magnetic equator over a large range in radial distance 1.5 - 4 R_E geocentric and that specific L shells for both positive and

negative B_z values (non-storm and storm conditions) have the highest intensities of the emission. Figure 1B shows that the most intense portion of the equatorial EM emissions is located in the mid to late afternoon local time region and that the emission is rarely measured in the pre-midnight sector. Previous results have left the impression that the EM equatorial emissions are observed at all local times.

2.2 PLASMASPHERIC HISS

The plasma wave magnetic spectral density maps for plasmaspheric hiss near its spectral peak between 1 and 2 kHz are shown in Figure 2. Although found essentially everywhere in the plasmasphere at some intensity, plasmaspheric hiss is most intense throughout the local afternoon sector (see Figure 2B) and on L shells which contain the slot region in the electron radiation belts (see Figure 2A). In the frequency range from ~330 Hz to ~3.3 kHz both meridian and X-Y plane plasma wave magnetic field spectral density maps from PWI data show essentially the same distributions as in Figure 2 for 1.2 kHz. Over the frequency range from 2.7 to 3.3 kHz the intensity and spatial extent of the emission decreases significantly. The transition from the EM equatorial emission to plasmaspheric hiss occurs over the frequency range from ~230 Hz to ~380 Hz. The wave activity in Figure 2B occurring in the early morning and near dawn sector is just the beginning of the chorus emissions that will be discussed in the next section.

It is important to note that in the frequency range from ~330 Hz to ~3.3 kHz that several emissions are observed in the plasmasphere such as plasmaspheric hiss, whistlers, and chorus. The DE/PWI instrument has a bandwidth of 1% and a time resolution of 1 second/32 channels, when combined with the wave map technique used in this study, the results are not sufficient to resolve the plasma wave observations into discrete whistlers. Whistlers are most commonly observed by wide-band instruments giving superior time and frequency resolution and typically automatic gain control all of which enable discrete emissions such as whistlers to be captured. Therefore, the results of this study, by their nature, emphasize observations of continuum-like spectra. The identification of the plasmaspheric hiss is uniquely done from the spatial distribution in magnetic latitude and

local time at each frequency. The similarity of this distribution over a number of consecutive frequency channels significantly supports the identification of the emission as plasmaspheric hiss.

It is important to note that these distributions are smoothed and by their nature would only show geomagnetic storm-time differences if the latitudinal structures changed significantly as in the case of the equatorial EM radiation of Figure 1. Since there is no significant change in the latitudinal distribution of plasmaspheric hiss, as shown in Figure 2, storm time intensifications that have been reported by *Larkina and Likhter* [1982] are therefore all averaged together.

The waves that *Thorne et al.* [1973] describe as plasmaspheric hiss that “appear to be continuously present throughout the plasmasphere at all latitudes and longitudes” may actually be a combination of both equatorial EM radiation and plasmaspheric hiss as described in this paper. Although similar in MLT distribution as shown in Figure 1B and 2B the latitudinal distributions (Figures 1A and 2A) show a significantly different distribution. It is only through this wave map technique that we are able to clearly distinguish between these two types of whistler mode radiation.

It is important to note that in the recent paper by *Meredith et al.* [2004] that wave maps of plasmaspheric hiss were generated by combining frequencies between 0.1 to 2 kHz and were analyzed as plasmaspheric hiss. We believe that their technique potentially combines some of the equatorial EM emissions with plasmaspheric hiss. As clearly demonstrated in this paper, the EM emissions dominate the spectrum in the frequency range up to ~330 Hz and have significantly different spatial distributions relative to plasmaspheric hiss and to substorm parameters (IMF B_z).

2.3 CHORUS

Whistler mode chorus observations are observed from near the plasmopause and to greater radial distances. Figure 3 is in the same format as Figure 1 but showing the

electric field intensity for 5.1 kHz. Panel A shows the whistler mode waves in the polar cusp (on the dayside at high L values), in the auroral zone (on the nightside) and in the magnetic equator on the nightside which are the chorus waves. The chorus emissions are further illustrated in panel B showing the broad spatial distribution extending from early morning hours to nearly noon. The distribution of chorus as shown in Figure 3 is nearly identical to that reported by *Tsurutani and Smith* [1979], *Koons and Roeder* [1990], and *Summers et al.* [1998]. Using the wave map technique similar spatial distributions of chorus extend from ~1.2 to ~6 kHz in frequency.

As discussed previously, chorus emissions are characterized as discrete emissions usually rising rapidly in frequency with time. Typically a large number of these discrete emissions are observed together and are often observed with a band of hiss emissions [*Koons*, 1981]. These two factors contribute to chorus emissions being clearly identified on a number of sweep frequency receiver systems [see for example: *Horne et al.*, 2003] in addition to wide-band instruments [*Santolik et al.*, 2004] and therefore allow us to be able to identify at least the most intense chorus distributions in the wave map study presented here.

2.4 GROUND TRANSMITTERS

VLF ground transmitters operate over the frequency range from ~10 to 50 kHz with a narrow bandwidth (usually < 1 kHz) and generate wave energy that typically couples into the plasmasphere in the whistler mode. Figure 4 is in the same format as Figure 1 and Figure 2, but for magnetic field spectral densities at 11.8 kHz, and with f_{ge} and f_{LHR} indicated by red and green lines, respectively. The distribution shown in this figure is similar to those at frequencies of all other ground transmitters from 10-50 kHz. Panel A shows the latitudinal distribution of the magnetic field spectral density of the waves that follow mid-latitude field lines. Panel B shows that the maximum magnetic field spectral density of waves from ground transmitters occurs on the nightside. It is important to note the similarity in the latitudinal distribution of plasmaspheric hiss (Figure 2) and that of

transmitters (Figure 4) even though the most intense portions of these waves have different local time distributions.

The electric field spectral densities from IMAGE/RPI of three ground transmitters operating in the US (two, NLK and NML, known to us; one unknown) at 25.0 kHz are shown in Figure 5. Panels A and C are data selected from the 14-18 MLT and 02-06 MLT sectors respectively as shown in panel B which is in the same local time distribution format as that presented at 11.5 kHz of Figure 4. The electric field wave measurements in panels A and C are mapped to geographic coordinates along the associated geomagnetic field lines. Electric field wave measurements within 10° of the magnetic equator or in locations in which the gyrofrequency was less than the wave frequency were excluded. This criteria was necessary to insure that only whistler mode waves were included and that the appropriate mapping along field-lines was accomplished to keep the northern and southern hemisphere distributions separate. The magnetic conjugate points of the transmitters are shown as white dots.

Figure 5 shows the broad, 10s of degrees extent of the transmitter radiation, which couples from the ground into the plasmasphere. The figure clearly shows that the transmitters' waves coupling into the plasmasphere are strongest on the night side (panel C) and weakest on the dayside (panel A) where the extent of the coupling is significantly less. In addition, the transmitter observations in Figure 5 shows the confinement of the whistler mode waves to a longitude range of about 30° to 40° on the day side (panel A) from its generation sites.

It has been known for sometime [Helliwell, 1965] that ionospheric absorption of VLF signals generated on the ground depends mainly upon the electron density and collision frequency (between electrons and neutrals) in the D layer. The D layer is the most extensive on the dayside since its dominant source is photoionization followed by precipitation (which is not significant at the mid-latitudes where the ground transmitters mostly reside). Given that ground transmitters generate a constant source of emission

with local time the differences in the day-night distribution shown in Figure 5 are most likely due to the day-night asymmetry in the absorbing D layer.

3. LIGHTNING AS A SOURCE OF PLASMASPHERIC HISS

The classic theoretical work by *Kenel and Petschek*, [1966] held that, under certain circumstances, whistler mode waves increase in energy from a gyroresonance interaction with radiation belt electrons causing the electrons to change pitch angle and precipitate (pitch angle scattering). *Lyons et al.* [1972] and *Abel and Thorne* [1998a,b] showed that plasmaspheric hiss would be the dominant whistler mode wave responsible for this scattering thereby maintaining the electron slot region between the inner and outer electron belts. Therefore, understanding the origin of hiss is of fundamental importance in understanding the distribution and dynamics of the electron radiation belts.

The origin of plasmaspheric hiss is still somewhat controversial as either generated by the above gyroresonance process [see for example: *Thorne et al.*, 1973; *Huang et al.*, 1983; *Church and Thorne*, 1983] or by lightning [*Sonwalker and Inan*, 1989; *Draganov et al.*, 1992] or both but the relative contribution from these two sources is still unknown even though the literature in this field is extensive. *Thorne et al.* [1979] suggested that plasmaspheric hiss would only grow in intensity from the background thermal noise to its observed intensity from gyroresonance acceleration as the whistler mode wave returned through the equator repeatedly. Based on limited data, *Solomon et al.* [1988] have shown that amplification of background noise to observed hiss intensities is possible. In addition, from ray tracing calculations of magnetospherically reflected whistlers, *Thorne and Horne* [1994] concluded that lightning generated whistlers could not be the source of plasmaspheric hiss because they are subject to significant damping due to Landau resonant interactions with suprathermal electrons with energies greater than about 100 eV.

Observations from the low frequency linear wave receiver on DE by *Sonwalker and Inan* [1989] have shown that lightning-generated whistlers often triggers plasmaspheric hiss.

These *in situ* observations were the first to demonstrate that lightning could be the original source of plasmaspheric hiss. Ray tracing calculations by *Draganov et al.* [1992] demonstrated that the refraction of the plasmasphere on lightning whistlers (higher frequencies waves move to higher L shells) produced a natural way to obtain a hiss like spectrum on lower L shells. In addition, *Draganov et al.* [1992] determined that the total wave energy from lightning whistlers may maintain the experimentally observed levels of plasmaspheric hiss.

The wave mapping technique used above in this study is applied over the frequency range from 30 Hz to 50 kHz. The transmitter data presented in section 2.4 is used to set the context for analyzing the whistler mode waves at lower frequencies. The similarities in Figures 2A (hiss) and 4A (transmitters), showing that the most intense portion of the waves are along high latitude magnetic field lines, suggest an Earth origin even though the local time distributions are different. These observations support the previous work by *Sonwalker and Inan* [1989] and *Draganov et al.* [1992] and provides the motivation to further explore the possibility of an Earth origin for hiss.

In order to investigate what contribution lightning may play in providing whistler mode radiation into the plasmasphere, DE/PWI (30 Hz to 50 kHz) and IMAGE/RPI (3 to 50 kHz) data, separately and at each frequency, were remapped into geographic coordinates and compared with the average distribution of lightning creating a whole new series of wave maps for analysis. Like the transmitter data of Figure 5, the electric field wave measurements within 10° of the magnetic equator or in locations in which the gyrofrequency was less than the wave frequency were excluded. The data prepared in this way would then provide insight into the importance of lightning as a source of plasmaspheric hiss. Plasmaspheric hiss that grows in intensity due to particle-wave interactions from the background thermal noise, as suggested by *Thorne et al.* [1979], would have a distribution completely independent of any geographic mapping. In order for lightning to be even considered to be an element of plasmaspheric hiss a geographic relationship would have to be established between lightning and the observed distribution of plasmaspheric hiss.

The average distribution of lightning strikes world-wide has been measured from the Optical Transient Detector on board the MicroLab-1 satellite by *Christian et al.* [2003] and is shown in Figure 6 along with the main slot region L shells [after *Rodger et al.*, 2003]. Figure 6 is an annualized distribution of lightning clearly showing that the lightning distributions are largely confined to the continents. Due to the tilt of the magnetic pole, the continents of North America, Europe, Russia, and Australia provide the vast majority of lightning whistlers into the slot region. *Christian et al.* [2003] also showed the seasonal lightning distributions (see their Figure 7). The seasonal distributions of lightning activity shows significantly more lightning in the summer hemisphere than in the corresponding winter hemisphere. For instance, virtually no lightning is observed in the northern hemisphere during the months of December, January, and February. From an analysis of their annual lightning distributions, *Christian et al.* [2003] determined that lightning occurs mainly over land areas, with an average land/ocean ratio of 10:1. Statistically, these authors found that there are an average of 44 (+/-5) lightning flashes occurring around the globe every second. In another recent study of lightning, *Mazany et al.* [2002] measured the day-night effect at mid-latitudes and found that as much as 10 times more lightning events occur in the post noon than in the post midnight sector.

The average wave electric field spectral density from all DE/PWI measurements of plasmaspheric hiss mapped to magnetic coordinates with continents, at 3 kHz, is shown in Figure 7 (in a similar manner as the transmitter data in Figure 5A and C). The left panels are dayside and the right panels, nightside. The top panels are summer and the bottom panels, winter. The equinox months of March and September are excluded. The analysis of the resulting wave maps shows that the correspondence between the enhanced intensities and continents occurs over the ~500 Hz to about 3 kHz frequency range. This is almost identical to the frequency range of plasmaspheric hiss as determined from the spatial distributions presented in this study (see section 2.2 and Figure 2).

Like the world distribution of lightning, the world distribution of plasmaspheric hiss follows the continents and is stronger on the dayside than the nightside and is stronger in summer than in winter. The same distributions are also observed with the IMAGE/RPI data. The day/night asymmetry can also be seen in Figure 2B.

Electric field spectral density measurements and the major landmasses from Figure 7 at 45° invariant latitude ($L=2$ slot region) in the northern hemisphere are shown in Figure 8. Figure 8 provides quantitative measurements of the average electric field and allows for direct comparison of the summer/winter and day/night effects that Earth lightning exhibits. The summer data is shown in red and the winter in blue. Peak intensities of plasmaspheric hiss are shown over land with minimums over the ocean with summer being stronger than the observations during the winter. The average variation between the red and blue curves in both panels A and B is approximately 1 order of magnitude. These results strongly suggest that lightning is the dominant source of plasmaspheric hiss.

The observations in Figure 5 of radiation from ground transmitters clearly shows peak intensities above the radiating stations and at their associated conjugate point. Assuming that waves from lightning also follow this pattern it is important to consider how the lightning from the southern hemisphere would effect these observations. The winter (northern hemisphere) trace in Figure 8A shows a clear wave intensity peak from -150° to -110° magnetic longitude. This peak corresponds to the conjugate longitude of Australia which is the only southern hemisphere continent on L shells that maps into the slot region and would be in its summer season where the peak in its thunderstorms occur. Once again this provides more confidence in lightning as the primary source of plasmaspheric hiss.

4. DISCUSSION

If lightning is a major source of plasmaspheric hiss, as this study indicates, why then are the discrete frequencies characteristic of a plasmaspheric lightning whistler so different than the broad, featureless, variable intensity characteristic of plasmaspheric hiss?

Draganov et al. [1992], used ray tracing calculations to demonstrate the evolution of

magnetospherically reflected whistler wave energy into hiss-like spectra, via the settling of wave energy on specific L-shells. Magnetospherically reflecting whistlers do not bounce off the plasmapause but are internally reflected within the plasmasphere. *Draganov et al.* [1992] found that the lightning-generated whistlers tend to settle on preferred L-shells in the plasmasphere with the lower frequency components settling at higher L-shells and higher frequency components on lower L-shells. Their estimates of the resulting whistler mode energy from lightning discharges were comparable to experimentally observed levels of plasmaspheric hiss. By combining the lightning whistler lifetimes with the power spectral density of lightning, *Bortnik et al.* [2003] showed a clear maximum in wave energy in the slot region at an L of about 2 - 3. This is very consistent with the observations presented in Figure 2A and 2B. *Sonwalker and Inan* [1989] observed that lightning-generated whistlers often trigger hiss emissions. These observations led the authors to the conclusion that lightning served, to an unknown extent, as an embryonic source of plasmaspheric hiss. This paper puts the above previous results into context and shows that lightning must be a major source of plasmaspheric hiss. Figure 8 shows the geographic mapping of plasmasphere hiss is strikingly similar to lightning distributions for both day/night and summer/winter variability. The evidence is compelling and overwhelming.

Previous researchers have tried to make the same connection. *Tsurutani et al.* [1979] searched for geographic dependence of plasmaspheric hiss at 550 Hz from the polar orbiting OGO 6. Their conclusion was that from the "totality of satellite data analyzed to date ...[the results are] consistent with a predominantly natural origin [non-lightning] for ... plasmaspheric hiss." It is unfortunate that these authors did not look at higher frequencies since the strong geographic mapping of plasmaspheric hiss only becomes obvious above this frequency.

The reason why the plasmaspheric hiss maps so well to the geography of land (Figures 6) is revealed by examining the day-night variation in longitude from the transmitter waves coupling into the plasmasphere (Figure 5). Unlike ground transmitters, the most intense portion of plasmaspheric hiss occurs on the dayside (afternoon sector) rather than on the

nightside. This matches the measured day-night asymmetry of lightning as reported by *Mazany et al.* [2002]. Lightning is much more frequent on the dayside but when it couples through into the plasmasphere it will be much more confined in longitude than lightning on the nightside. The nightside distributions (Figure 8B) still show the peak average spectral power density corresponding to land but they are broader in longitudinal extent showing less of a correspondence to land than on the dayside (panel A) as would be expected from the transmitter analogy (Figure 4).

The intensity of plasmaspheric hiss has been observed to be higher near the magnetic equator during substorm conditions [*Larkina and Likhter*, 1982]. The results of this study shows that no significant changes in the latitudinal distribution of plasmaspheric hiss occurs (see Figure 2A) with IMF B_z positive or negative which is the substorm parameter we chose to use. Therefore, this effect is not obvious in the wave map technique used in this study since average electric field spectra were used here. This implies that the mechanism responsible for the increase in the storm time hiss intensities (most likely the Kennel-Petschek mechanism) must be operating primarily in the slot region all the time at some level. During quiet periods the radiation belts come into equilibrium with the plasmaspheric hiss revealing a slot region between the two Van Allen belts. However, during very strong geomagnetic storms this slot region can be filled with energetic particles. Even with the constant supply of lightning providing wave energy for the resonance interaction it can take up to 3 or more days for the belts to recover back to their normal equilibrium of a two belt configuration.

Electrons, in the energy range from 100-300 keV, have been observed by the Stimulated Emission of Energetic Particles (SEEP) experiment on the S81-1 satellite to precipitate by lightning-generated whistlers as reported by a number of authors [*Voss et al.*, 1984; *Inan et al.*, 1989; *Voss et al.*, 1998]. More recently, *Rodger et al.* [2003] determined, from modeling calculations, that electrons in the ~50 to 150 keV energy range can precipitate out of the slot region ($L = 2 - 2.4$) through gyroresonance interaction with lightning generated whistlers as the dominant wave. The whistler distribution used by *Rodger et al.* [2003] was based on lightning climatology maps from *Christian et al.*

[2003]. For electron energies above this range, *Rodger et al.* [2003] believe that ground-based transmitters and plasmaspheric hiss should dominate over all other loss processes. The results of our study is consistent with these conclusions based on actual observations of the distribution of plasmaspheric hiss that has lightning as its origin.

5. CONCLUSIONS

From the analysis of plasma wave intensity maps from the DE/PWI and IMAGE/RPI instruments this paper puts in context a number of previous observations and proposed generation mechanisms of whistler mode waves in the plasmasphere. The whistler mode spectrum in the plasmasphere contains three basic broadband waves: equatorial EM emissions (~ 10 Hz – 330 Hz), plasmaspheric hiss (~ 330 – 3.3 kHz), and ground transmitter radiation (~ 10 -50 kHz). Each of these waves is easily distinguishable by their spatial distributions in both local time and longitude. Figure 9 is a summary of where these waves are most intense in local time.

Observations of EM equatorial emissions show that the most intense region is near the magnetic equator in the noon to afternoon sector. This emission is enhanced during storm times as illustrated by its dependence on the IMF B_z (see Figure 1). The observed average magnetic field spectral densities have latitudinal distributions that are very different from plasmaspheric hiss and ground transmitters and show an almost exclusive plasmasphere origin with lightning having little, if anything, to do with the intensity of this emission.

The mapping of plasmaspheric hiss over nearly its entire frequency range (starting at ~ 500 Hz to over 3 kHz) from L shells greater than 1.5 to geographic longitudes shows a number of features identical to that of lightning. The most intense plasmaspheric hiss is mapped to northern hemispheric continents (weakest hiss over oceans), stronger on the dayside than on the nightside, and stronger during the summer than winter. The difference in average hiss intensity between the land and ocean is greater than an order of magnitude and therefore comparable to that of the distribution of lightning. In addition,

from wave intensity maps, the high latitude/low altitude distribution of plasmaspheric hiss is identical to that of known ground transmitters which clearly have an Earth origin. The above strong correlation between regions of lightning and regions of hiss make it clear that lightning is an embryonic source for hiss as originally suggested by *Sonwalker and Inan*, [1989]. However, it is not possible to determine if lightning is the sole source of plasmaspheric hiss as proposed by *Draganov et al.*, [1992].

It is important to also note that a clear intensification of hiss also occurs near the magnetic equator where particle-wave interactions, most likely generated by the *Kennel and Petschek* [1966] mechanism occurs. With lightning maintaining the average hiss intensity in the slot region, the Kennel-Petschek mechanism must increase the hiss intensity during storm conditions as has recently been discussed by *Larkina and Likhter*, [1982] and *Meredith et al.* [2004].

Ground transmitter waves have narrow bandwidths (typically <1 kHz) and couple through the ionosphere primarily on the night side. From ~10 to 50 kHz whistler mode waves, observed by IMAGE/RPI (bandwidth 300 Hz), greatly fill in the spectrum between non-transmitter frequencies with the implication that some unknown process is broadening the spectrum.

Acknowledgments. The authors gratefully acknowledge discussions with Umran Inan and Richard Thorne. The data used in this paper are from the National Space Science Data Center archive. NASA supported the work at the University of Massachusetts, Lowell under subcontracts to Southwest Research Institute under contract NASW-97002. The authors would also like to acknowledge the reviewers for their excellent remarks and suggestions.

REFERENCES

- Abel, B., and R. M. Thorne, Electron scattering loss in Earth's inner magnetosphere: 1. Dominant physical processes, *J. Geophys. Res.*, *103*, 2385-2396, 1998a.
- Abel, B., and R. M. Thorne, Electron scattering loss in Earth's inner magnetosphere: 2. Sensitivity to model parameters, *J. Geophys. Res.*, *103*, 2397-2407, 1998b.
- André, R., F. Lefeuvre, F. Simonet, and U. S. Inan, A first approach to model the low-frequency wave activity in the plasmasphere, *Annales Geophys.*, *20*, 981-996, 2002.
- Boardsen, S. A., D. L. Gallagher, D. A. Gurnett, W. K. Peterson, and J. L. Green, Funnel-shaped, low frequency equatorial waves, *J. Geophys. Res.*, *97*, 14967-14976, 1992.
- Bortnik, J., U. S. Inan, and T. F. Bell, Energy distribution and lifetime of magnetospherically reflecting whistlers in the plasmasphere, *J. Geophys. Res.*, *108*(A5), 1199, doi:10.1029/2002JA009316, 2003.
- Christian, H. J., R. J. Blakeslee, D. J. Boccippio, W. L. Boeck, D. E. Buechler, K. T. Driscoll, S. J. Goodman, J. Hall, W. Koshak, D. Mach, and M. Stewart, Global frequency and distribution of lightning as observed from space by the Optical Transient Detector, *J. Geophys. Res.*, *108*, doi:10.1029/2002JD002347, 2003.
- Church, S. R., and Thorne, R. M., On the origin of plasmaspheric hiss: Ray path integrated amplification, *J. Geophys. Res.*, *88*, 7941-7957, 1983.
- Draganov, A. B., U. S. Inan, V. S. Sonwalkar, and T. F. Bell, Magnetospherically reflected whistlers as a source of plasmaspheric hiss, *Geophys. Res. Lett.*, *19*, 233-236, 1992.
- Dunckel, N., and R. A. Helliwell, Whistler-mode emissions on the Ogo 1 satellite, *J. Geophys. Res.*, *74*, 6371-6385, 1969.
- Green, J. L., and S. A. Boardsen, Confinement of non-thermal continuum radiation to low latitudes, *J. Geophys. Res.*, *104*, 10307-10316, 1999.
- Gurnett, D. A., Plasma wave interactions with energetic ions near the magnetic equator, *J. Geophys. Res.*, *81*, 2765-2770, 1976.
- Hayakawa, M., and S. S. Sazhin, Mid-latitude and plasmaspheric hiss: a review, *Planet Space Sci.*, *40*, 1325, 1992.
- Helliwell, R. A., "Whistlers and Related Ionospheric Phenomena," Stanford University Press, pp. 61-72, 1965.

- Horne, R. B., N. P. Meredith, R. M. Thorne, D. Heynderickx, R. H. A. Iles, and R. R. Anderson, Evolution of energetic electron pitch angle distributions during storm time electron acceleration to megaelectronvolt energies, *J. Geophys. Res.*, *108*(A1), 1016, doi:10.1029/2001JA009165, 2003.
- Huang, C. Y., C. K. Goertz, and R. R. Anderson, A theoretical study of plasmaspheric hiss generation, *J. Geophys. Res.*, *88*, 7927-7940, 1983.
- Imhof, W., R. R. Anderson, J. Reagan, and E. Gaines, The significance of VLF transmitters in the precipitation of inner belt electrons, *J. Geophys. Res.*, *86*, 11225-11234, 1981.
- Inan, U. S. and R. Helliwell, DE-1 observations of VLF transmitter signals and wave particle interactions in the magnetosphere, *Geophys. Res. Lett.*, *9*, 917-920, 1982.
- Inan, U. S., M. Walt, H. D. Voss, and W. L. Imhof, Energy spectra and pitch angle distributions of lightning-induced electron precipitation: Analysis of an event observed on the S81-1 (SEEP) satellite, *J. Geophys. Res.*, *94*, 1379-1401, 1989.
- Kennel, C. F., and H. E. Petschek, Limit on stably trapped particle fluxes, *J. Geophys. Res.*, *71*, 1-28, 1966.
- Koons, H. C., The role of hiss in magnetospheric chorus emissions, *J. Geophys. Res.*, *86*, 6745-6754, 1981.
- Koons, H. and Roeder, J, A survey of equatorial magnetospheric wave activity between 5 and 8 R_E , *Planet. Space Sci.*, *38*, 1335, 1990.
- Larkina, V. I., and Ja. I. Likhter, Storm-time variations of plasmaspheric ELF hiss, *J. Atmos. and Terr. Phys.*, *44*, 415-423, 1982.
- Lyons, L. R., R. M. Thorne, and C. F. Kennel, Pitch-angle diffusion of radiation belt electrons within the plasmasphere, *J. Geophys. Res.*, *77*, 3455-3474, 1972.
- Mazany, R, S. Businger, S.I. Gutman, and W. Roeder, A lightning prediction index that utilizes GPS integrated precipitable water vapor. *Weather and Forecasting*, *17*, 1034-1047, 2002.
- Meredith, N. P., R. B. Horne, A. D. Johnstone, and R. R. Anderson, The temporal evolution of electron distributions and associated wave activity following substorm injections in the inner magnetosphere, *J. Geophys. Res.*, *105*, 12907-12917, 2000.

- Meredith, N. P., R. B. Horne, R. H. A. Iles, R. M. Thorne, D. Heynderickx, and R. R. Anderson, Outer zone relativistic electron accelerations associated with substorm enhanced whistler mode chorus, *J. Geophys. Res.*, *107*(A7), 114, doi:10.1029/2001JA900146, 2002.
- Meredith, N. P., R. B. Horne, R. M. Thorne, D. Summers, and R. R. Anderson, Substorm dependence of plasmaspheric hiss, *J. Geophys. Res.*, *109*, A06209, doi:10.1029/2004JA010387, 2004.
- Reinisch, B. W., D. M. Haines, K. Bibl, G. Cheney, I. A. Galkin, X. Huang, S. H. Myers, and G. S. Sales, R. F. Benson, S. F. Fung, J. L. Green, W. W. L. Taylor, J.-L. Bougeret, R. Manning, N. Meyer-Vernet, and M. Moncuquet, D. L. Carpenter, D. L. Gallagher, and P. Reiff, The Radio Plasma Imager investigation on the IMAGE spacecraft, *Space Science Reviews*, *91*, 319-359, 2000.
- Rodger, C. J., M. A. Cilverd, and R. J. McCormick, Significance of lightning-generated whistlers to inner radiation belt electron lifetimes, *J. Geophys. Res.*, *108*(A12), 1462, doi:10.1029/2003JA009906, 2003.
- Russell, C. T., R. E. Holzer, and E. J. Smith, OGO 3 observations of ELF noise in the magnetosphere: 1. Spatial extent and frequency of occurrence, *J. Geophys. Res.*, *74*, 755-777, 1969.
- Russell, C. T., R. E. Holzer, and E. J. Smith, OGO 3 observations of ELF noise in the magnetosphere, 2. The nature of the equatorial noise, *J. Geophys. Res.*, *75*, 755-768, 1970.
- Santolik, O., D. A. Gurnett, J. S. Pickett, M. Parrot, N. Cornilleau-Wehrin, A microscopic and nanoscopic view of storm-time chorus on 31 March 2001, *Geophys. Res. Lett.*, *31*, L02801, doi:10.1029/2003GL018757, 2004.
- Sazhin, S. S. and M. Hayakawa, Magnetospheric chorus emissions: A review, *Planet. Space Sci.*, *40*, 681, 1992.
- Shawhan, S. D., D. A. Gurnett, D. L. Odem, R. A. Helliwell and C. G. Park, The plasma wave and quasi-static electric field instrument (PWI) for Dynamics Explorer-A, *Space Sci. Instr.*, *5*, 535-550, 1981.

- Solomon, J., N. Cornilleau-Wehrlin, A. Korth, and G. Kremser, An Experimental study of ELF/VLF hiss generation in the Earth's magnetosphere, *J. Geophys. Res.*, *93*, 1839-1847, 1988.
- Sonwalker, V. S., and U. S. Inan, Lightning as an embryonic source of VLF hiss, *J. Geophys. Res.*, *94*, 6986-6994, 1989.
- Stix, T. H., *Waves in Plasmas*, AIP Press, New York, p. 27-28, 1992.
- Storey, L. R. O., An investigation of whistling atmospherics, *Phil. Trans. Roy. Soc.*, *246*, 113-141, 1953.
- Summers, D., R. M. Thorne, F., Xiao, Relativistic theory of wave-particle resonant diffusion with application to electron acceleration in the magnetosphere, *J. Geophys. Res.*, *103*, 20487-20500, 1998.
- Taylor, W. W. L., and D. A. Gurnett, The morphology of VLF emissions observed with the Injun 3 satellite, *J. Geophys. Res.*, *73*, 5615-5626, 1968.
- Thorne, R. M., E. J. Smith, R. K. Burton, and R. E. Holzer, Plasmaspheric hiss, *J. Geophys. Res.*, *78*, 1581-1595, 1973.
- Thorne, R. M., and J. N. Barfield, Further observational evidence regarding the origin of plasmaspheric hiss, *Geophys. Res. Letts.*, *3*, 29-32, 1976.
- Thorne, R. M., S. R. Church, and D. J. Gorney, On the origin of plasmaspheric hiss: the importance of wave propagation and the plasmopause, *J. Geophys. Res.*, *84*, 5241-5247, 1979.
- Thorne, R. M., and R. B. Horne, Landau damping of magnetospherically reflected whistlers, *J. Geophys. Res.*, *99*, 17249-17258, 1994.
- Tsurutani, B. T., S. R. Church, and R. M. Thorne, A search for geographic control on the occurrence of magnetospheric ELF emissions, *J. Geophys. Res.*, *84*, 4116-4124, 1979.
- Tsyganenko, N. A., Modeling the Earth's magnetospheric magnetic field confined within a realistic magnetopause, *J. Geophys. Res.*, *100*, 5599-5612, 1995.
- Vampola, A., VLF transmission induced slot electron precipitation, *Geophys. Res. Lett.*, *4*, 569-572, 1977.
- Voss, H. D., W. L. Imhof, J. Mobilia, E. E. Gaines, M. Walt, U. S. Inan, R. A. Helliwell, D. L. Carenter, J. P. Katsufakis, and H. C. Chang, Lightning-induced electron precipitation, *Nature*, *312*, 740, 1984.

Voss, H. D., M. Walt, W. L. Imhof, J. Mobilia, and U. S. Inan, Satellite observations of lightning-induced electron precipitation, *J. Geophys. Res.*, 103, 11725-11744, 1998.

Figure Captions

Figure 1. The latitudinal (panel A) and local time (panel B) distribution of the average magnetic field spectral density of equatorial EM emissions in the plasmasphere. Closed L shells of 1.5, 3, and 4 are shown in Panel A along with field lines at 70° , 75° , and 80° .

Figure 2. In the same format as Figure 1, but primarily for plasmaspheric hiss. Panel A shows the latitudinal distribution of the maximum intensity of the waves follows mid-latitude field lines. Panel B shows that the maximum intensity of plasmaspheric hiss occurs on the dayside. The emissions on the morning side are chorus.

Figure 3. In the same format as Figure 1 but showing the electric field intensity for 5.1 kHz. Panel A shows the whistler mode waves in the polar cusp (on the dayside at high L values), in the auroral zone (on the nightside) and in the magnetic equator on the nightside (chorus). The chorus emissions are further illustrated in panel B showing the broad spatial distribution extending from early morning hours to nearly noon.

Figure 4. In the same format as Figure 1, but for ground transmitters at 11.8 kHz. The intensity distribution shown in this figure is similar to all ground transmitters over the frequency range from ~ 10 to 50 kHz. Panel A shows the latitudinal distribution of the maximum intensity of the waves following mid-latitude field lines. Panel B shows that the maximum intensity of ground transmitters occurs on the nightside in the late evening and early morning sector.

Figure 5. The average electric field wave spectral density from IMAGE/RPI measurements of several ground transmitters at 25.0 kHz. The panel B shows the same basic local time distribution as that presented at 11.8 kHz of Figure 4. Panel C (02-06 MLT) and panel A (14-18 MLT) panels show the electric field wave measurements mapped to magnetic coordinates (with continents outlines) along field lines. Electric field wave data that was within 10° of the magnetic equator or in locations in which the gyrofrequency was less than the wave frequency were excluded. Three ground

transmitters are operating in the US. (two known; one unknown). The conjugate points of the known transmitters are shown as white dots. Transmitter radiation coupling from the atmosphere to the plasmasphere is the strongest on the night side (panel C).

Figure 6. The annualized geographic distribution of lightning from *Christian et al.* [2003] and the main slot region L shells after *Rodger et al.* [2003]. Due to the tilt of the magnetic pole, the continents of North America, Europe, Russia, and Australia provide the vast majority of lightning whistlers into the slot region.

Figure 7. The average electric wave spectral density from all DE/PWI data of plasmaspheric hiss mapped to geographic coordinates (in the same manner as Figure 5) at 3 kHz. The left panels are dayside and the right panels, nightside observations. The top panels are summer and bottom panels are winter with the exclusion of the equinox months March and September. Like the world distribution of lightning, the world distribution of plasmaspheric hiss follows the continents and is stronger on the dayside than the nightside and is stronger in summer than in winter. The same distributions are also observed with the IMAGE/RPI data.

Figure 8. Electric field spectral density measurements and landmasses at 45° invariant latitude of data sorted in Figure 7. The summer data is shown in red and the winter in blue. Peak intensities of plasmaspheric hiss are over land with minimums over the ocean with summer intensities being stronger than winter.

Figure 9. A summary of the local time distribution of the most intense portions of equatorial EM emissions, plasmaspheric hiss, and ground transmitters.

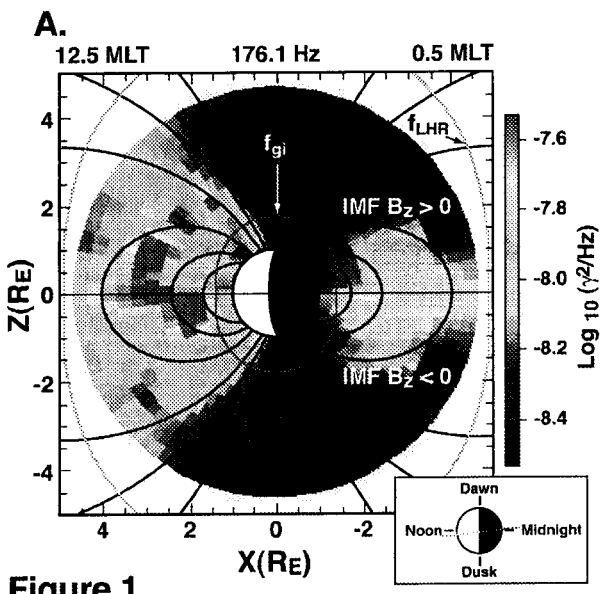
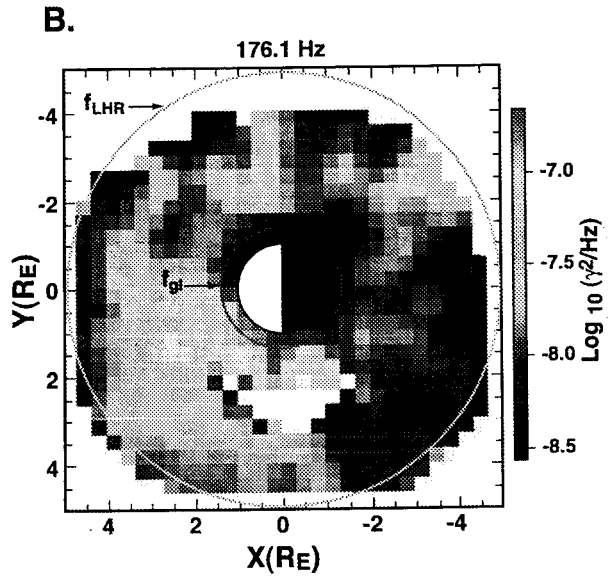


Figure 1



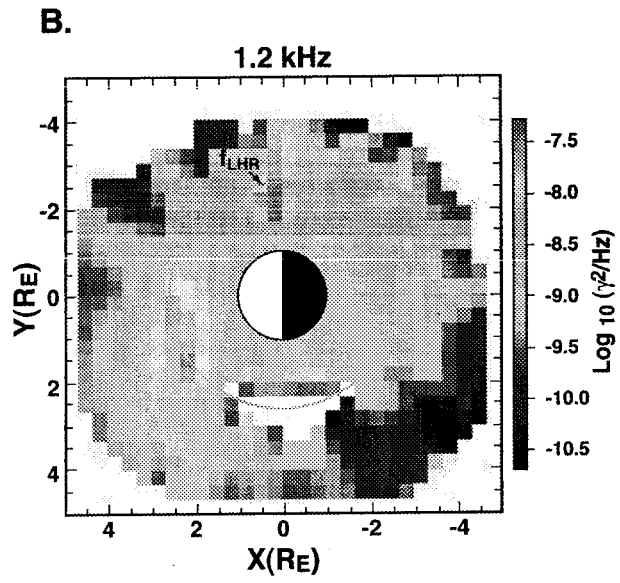
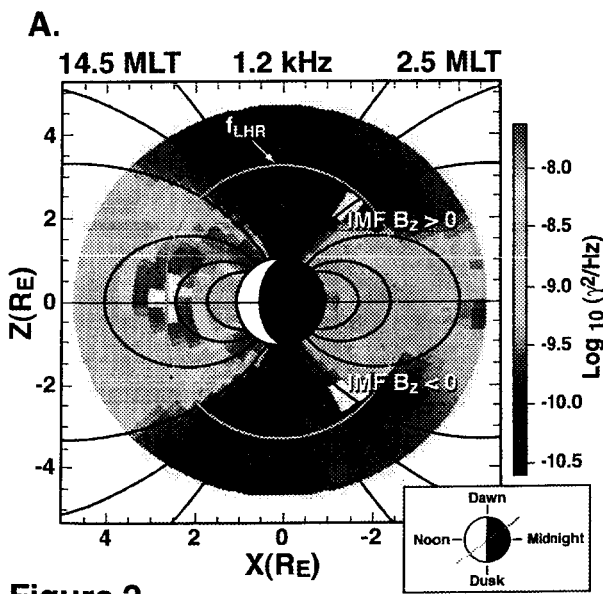


Figure 2

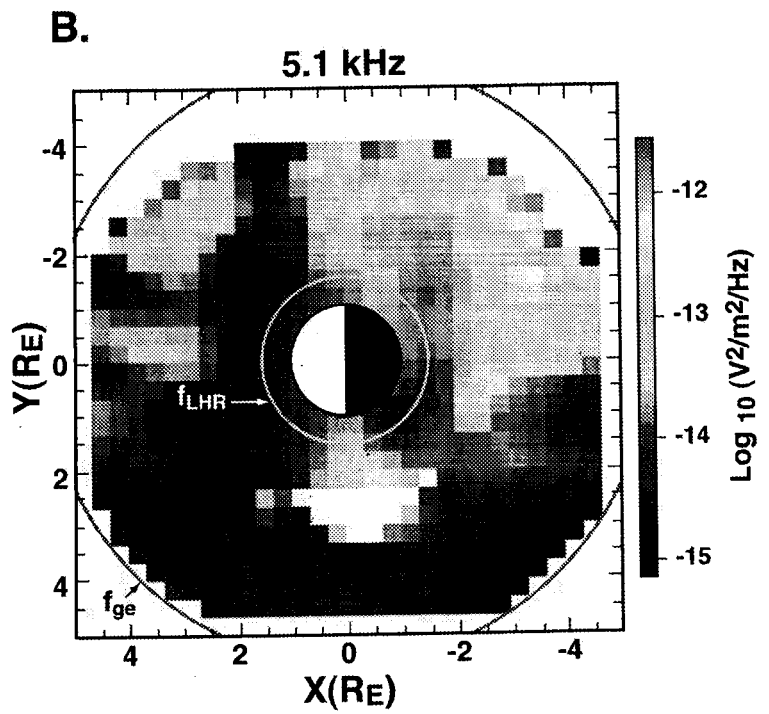
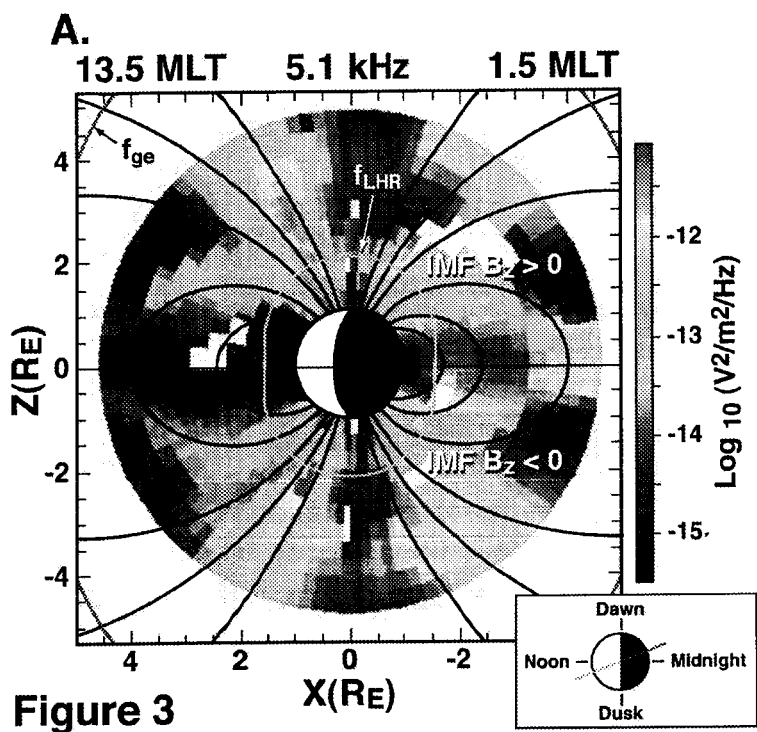


Figure 3

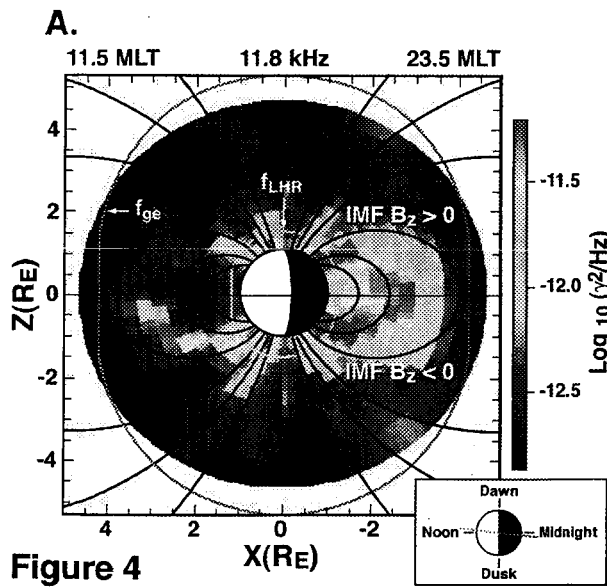
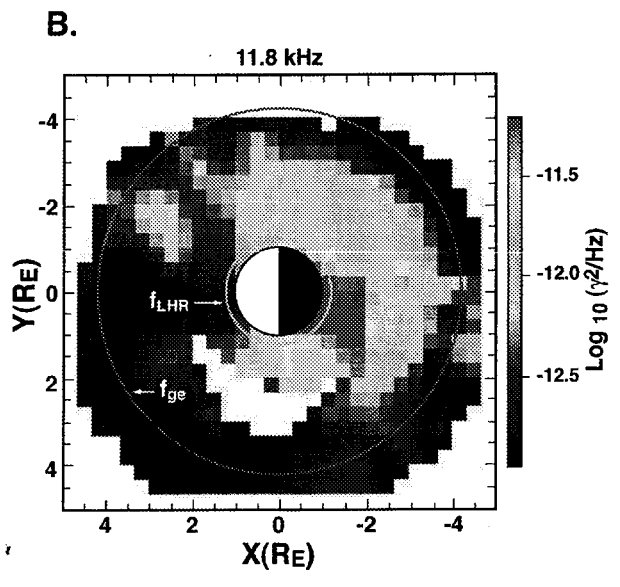


Figure 4



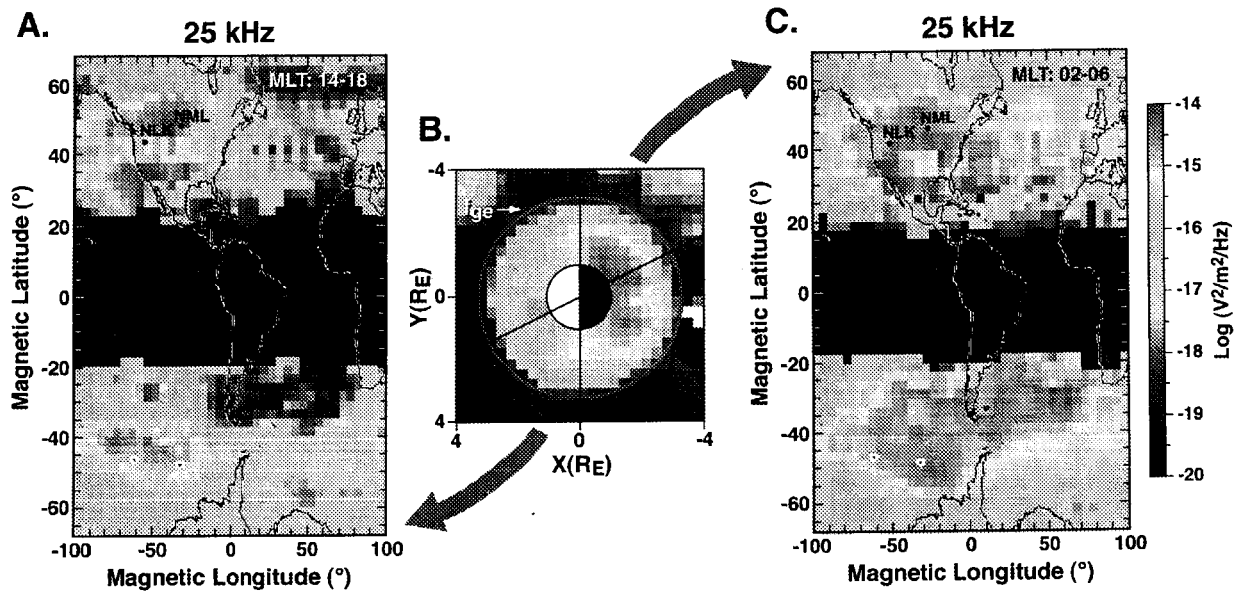


Figure 5

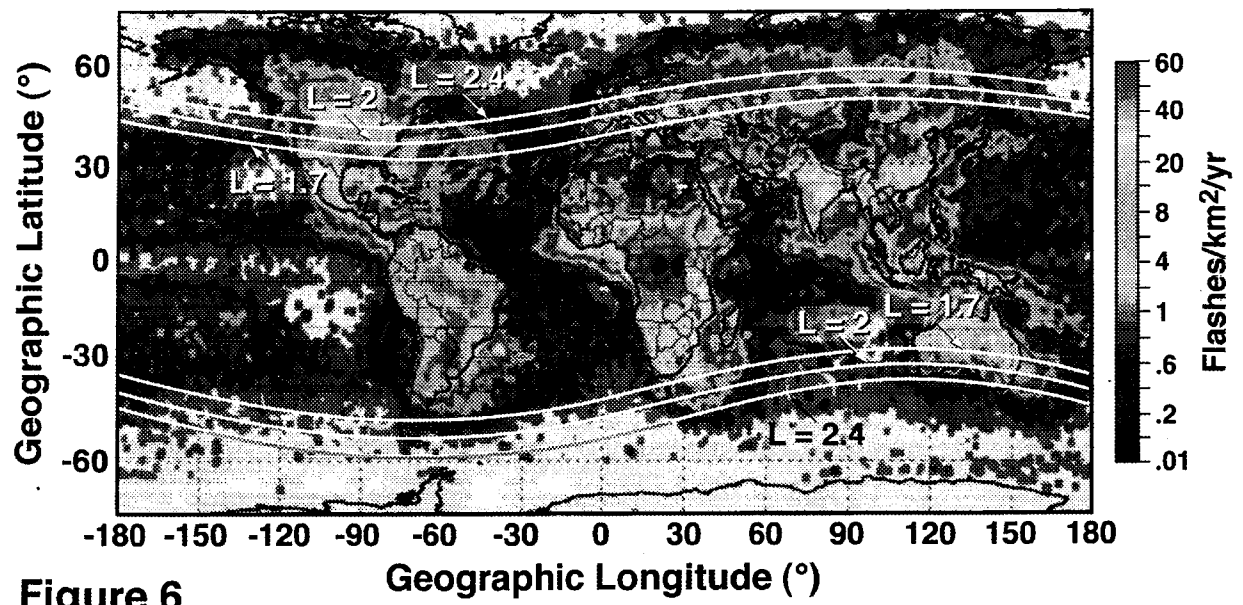


Figure 6

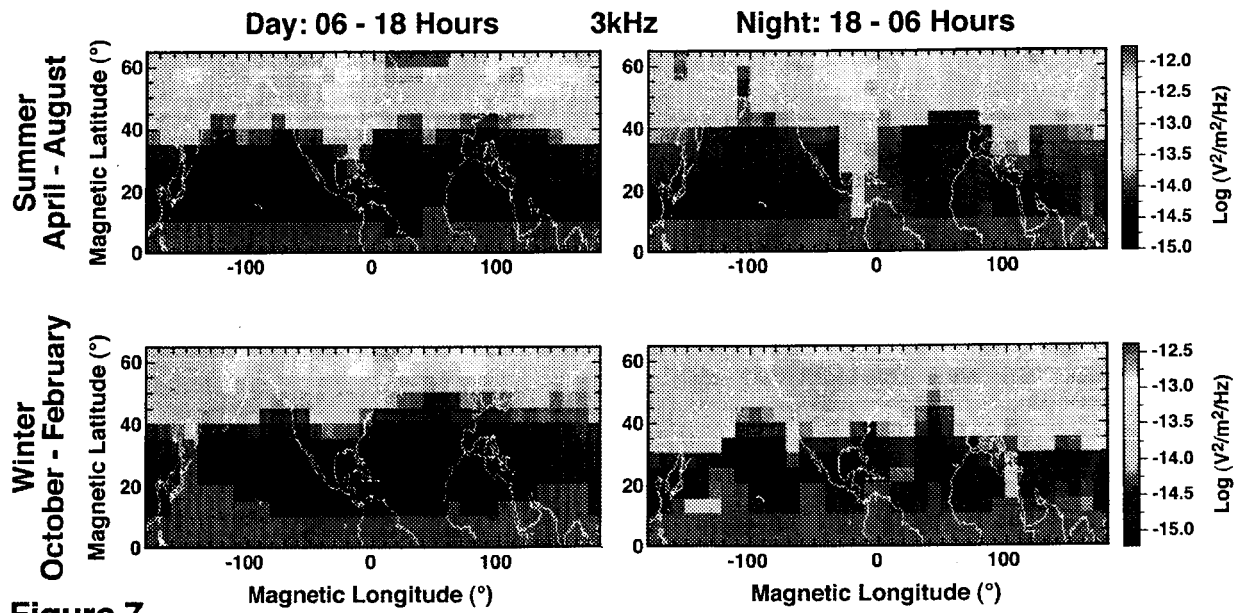


Figure 7

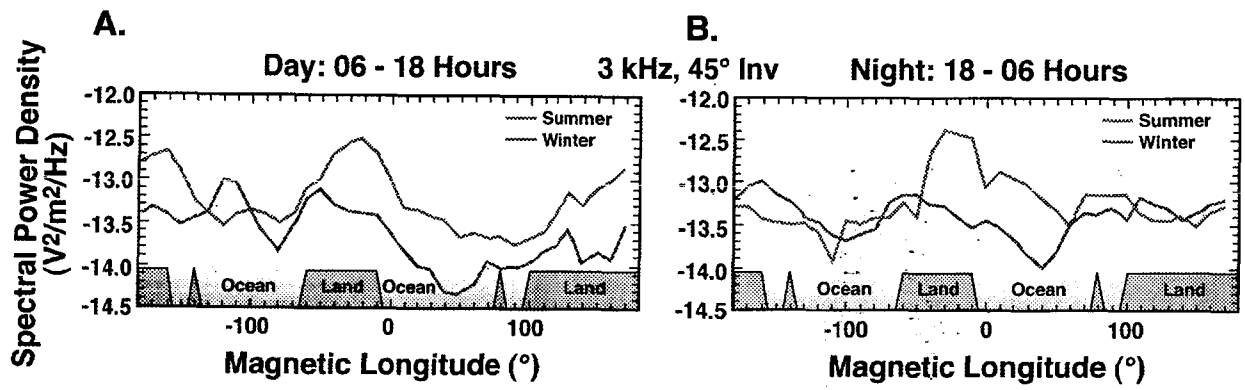


Figure 8

Whistler Mode Waves in the Plasmasphere

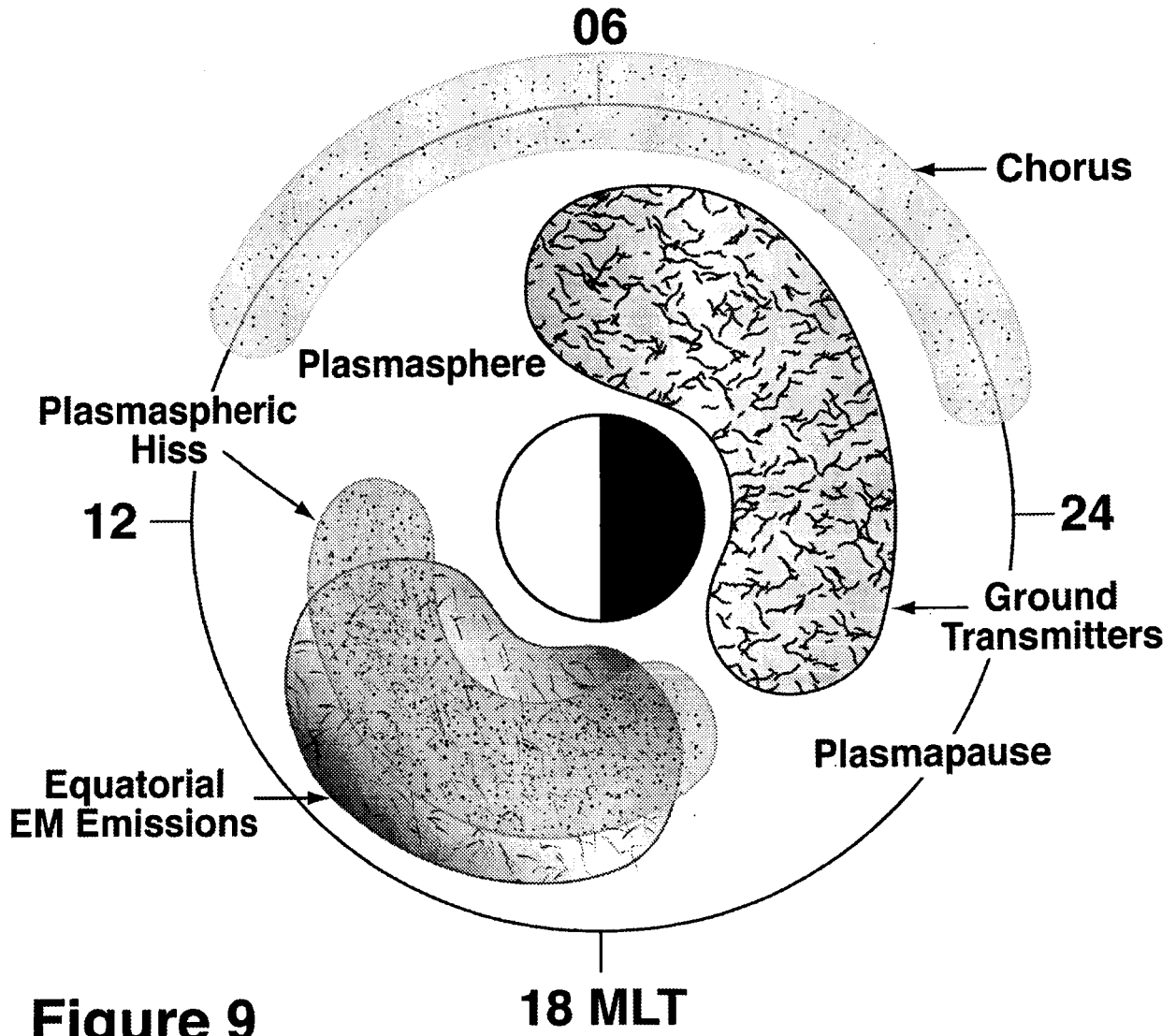


Figure 9